JACS
JOURNAL OF THE AMERICAN CHEMICAL SOCIETY
Communication
pubs.acs.org/JACS

Thieno-Pyrrole-Fused 4,4-Difluoro-4-bora-3a,4a-diaza-*s*-indacene–Fullerene Dyads: Utilization of Near-Infrared Sensitizers for Ultrafast Charge Separation in Donor–Acceptor Systems

Venugopal Bandi,[†] Sushanta K. Das,[†] Samuel G. Awuah,[‡] Youngjae You,*[,‡] and Francis D'Souza*[,†]

[†]Department of Chemistry, University of North Texas, 1155 Union Circle, #305070, Denton, Texas 76203-5017, United States
[‡]Department of Pharmaceutical Sciences, University of Oklahoma Health Sciences Center, 1110 N. Stonewall Avenue, Oklahoma City, Oklahoma 73117, United States

Supporting Information

ABSTRACT: Donor–acceptor dyads featuring near-IR sensitizers derived from thieno-pyrrole-fused BODIPY (abbreviated as SBDPiR) and fullerene, C_{60} have been newly synthesized and characterized. Occurrence of ultrafast photoinduced electron transfer (PET) leading to the formation of charge-separated state in these dyads, capable of harvesting light energy from the near-IR region, is established from femtosecond transient absorption studies.

The majority of the photosensitizers used in building donor–acceptor hybrids for light-to-electricity and light-to-fuel conversion, so-called artificial photosynthesis, either lack absorption or reveal inefficient electron transfer efficiency in the red and the near-infrared (near-IR) regions of the electromagnetic spectrum[1−11] (except for a few π-expanded phthalocyanine derivatives[8−10] and squaraine compounds[10−13]), which represents more than 70% of the solar spectrum. The primary reason for this limitation is in molecular engineering of such sensitizers in regulating their HOMO–LUMO gap such that they can harvest most of the photons from the near-IR regions, including part of the red region. Primary criterion includes maintaining the LUMO of the sensitizer above the LUMO level of the acceptor or the acceptor HOMO level above the donor HOMO level to furnish thermodynamically efficient excited state electron transfer.[10] Additionally, near-IR sensitizer development often requires tedious multistep synthesis, low reaction yields, reactive intermediates, poor solubility, poor photostability, and limited functionalization options.

The 4,4-difluoro-4-bora-3a,4a-diaza-*s*-indacene (BODIPY) is a very well-known molecule for its synthetic advantages in addition to its photostability, sharp absorption and emission, high molar absorptivity properties, and facile tuning of excited states.[14] Chemical modifications to the dipyrromethene core as well as functionalization to the boron center and the meso positions make BODIPYs adaptable for numerous applications, including protein-labeling fluorophores,[15] photosensitizers for photodynamic therapy (PDT),[16,17] and development of artificial photosynthetic model compounds.[18−21] In the present study, we have utilized the BODIPY molecular framework to develop near-IR absorbing and emitting thieno-pyrrole-fused BODIPY to construct novel donor–acceptor dyads involving fullerene, C_{60}, as an electron acceptor. As shown here, the newly constructed dyads undergo ultrafast PET leading into charge separation.

The structures of the near-IR sensitizer probes along with the dyads are shown in Chart 1, while the synthetic details are given in the Supporting Information. The synthesis involved (i) building a reactive brominated BODIPY electrophile having absorption in the visible region (635 nm) as an intermediate,[20] (ii) functionalization of the reactive BODIPY intermediate via transition metal-catalyzed coupling and nucleophilic substitution reactions,[22] (iii) converting the BF_2-chelated macrocycle to formyl phenyl dioxyboron derivative by reacting it with 3,4-dihydroxybenzaldehyde in the presence of $AlCl_3$,[23,24] and (iv) covalent linking of fullerene by reacting the formyl derivatives with fullerene and *N*-methylglycine (Scheme 1).[25] The newly synthesized dyads were fully characterized by spectral, mass, and electrochemical methods (see Figures S1–S5 in the Supporting Information).

Chart 1. Structure of the Newly Synthesized SBDPiR-C_{60} Dyads (SBDPiR = Thieno-Pyrrole-Fused BODIPY)[a]

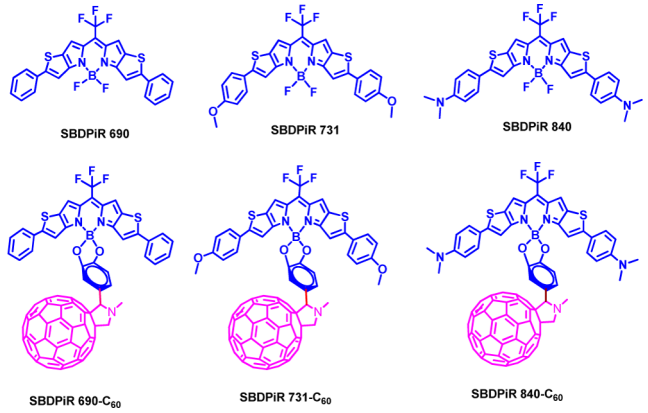

[a]The abbreviations 690, 731, and 840 refer to the absorption wavelength maxima of the near-IR sensitizers.

Received: March 25, 2014
Published: May 10, 2014

   dx.doi.org/10.1021/ja503015f | *J. Am. Chem. Soc.* 2014, 136, 7571–7574

Scheme 1. Synthetic Scheme of SBDPiR-Fullerene Dyads

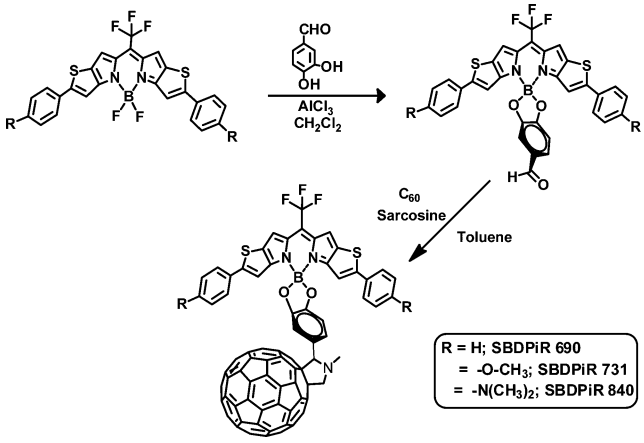

As shown in Figure 1a, the combination of thieno-pyrrole fusion and substituents on the 2-position of thieno ring

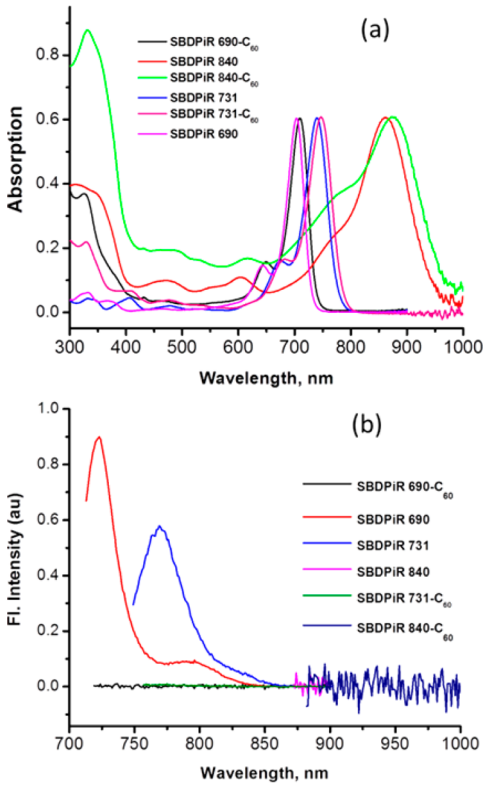

Figure 1. (a) Optical absorbance, normalized to the intense visible band, (b) fluorescence emission spectra of precursor, thieno-pyrrole-fused BODIPYs and the dyads formed by covalent attached of fullerene in benzonitrile. The compounds were excited at the respective peak maxima. The 875−1000 nm range was expanded (10×) for clarity.

extended the wavelength of absorption of BODIPY well into the near-IR region. Further, appending C_{60} through the boron center caused an additional red shift of 5−12 nm. The characteristic sharp peak of fulleropyrrolidine at 430 nm in all of the dyads was also observed. The fluorescence emission spectrum of SBDPiR 690 revealed an emission peak at 722 nm with a shoulder band at 795 nm when excited at 690 nm in benzonitrile (Figure 1b). Similarly, SBDPiR 731 revealed a band at 770 nm with a shoulder band at 829 nm.

The fluorescence lifetime of the SBDPiR 690 and SBDPiR 731 sensitizers evaluated from time-correlated singlet photon counting was found to be 1.55 (±0.02) ns and 3.22 (±0.02) ns, respectively. However, no emission for SBDPiR 840 was observed due to the presence of two *N*,*N*-dimethylaminophenyl entities which would promote intramolecular electron transfer (vide infra). Notably, upon appending fullerene to form the donor−acceptor dyads, quantitative quenching of fluorescence in all three dyads was witnessed, indicating the occurrence of photoinduced intramolecular events (Figure 1b). Energy transfer as a quenching mechanism was ruled out due to the absence of spectral overlap between SBDPiR emission and C_{60} absorption.

In order to visualize the geometry and the electronic structures of the dyads, ground state optimization of these dyads at the B3LYP/3-21G(*) level with Gaussian 03[26] were performed. As shown in Figure 2 (panels a−c), all of the dyads

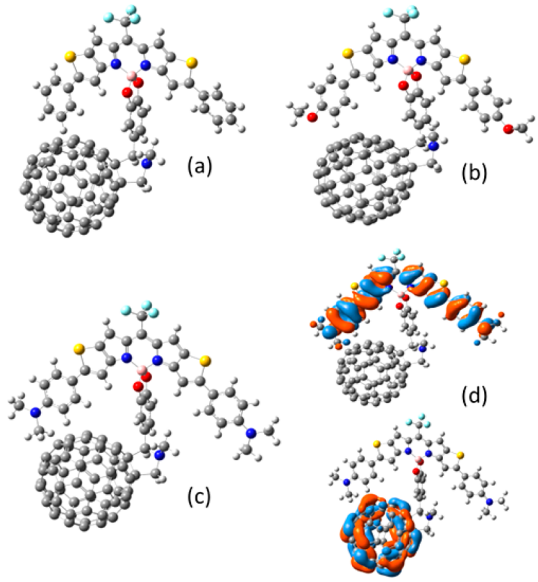

Figure 2. B3LYP/3-21G(*) optimized structures of (a) SBDPiR 690-C_{60}, (b) SBDPiR 731-C_{60}, and (c) SBDPiR 840-C_{60}. (d) HOMO and LUMO of SBDPiR 840-C_{60}.

revealed stable structures on the Born−Oppenheimer potential energy surface with no steric constraints between the donor and acceptor entities. The center-to-center distance between the boron atom and the center of the fullerene was found to be ∼9.9 Å, indicating close proximity of the donor and acceptor entities. As shown in Figure 2d, in the optimized structure of the SBDPiR 840-C_{60} dyad, the HOMO was located on the SBDPiR 840 entity while the LUMO was located on fullerene entity. Interestingly, for SBDPiR 690-C_{60} and SBDPiR 731-C_{60} dyads, the LUMO was on the SBDPiR macrocycle, while the LUMO+1 was on the fullerene entity and the HOMO on the SBDPiR entities (see Figure S6). The presence of LUMO on SBDPiR is suggestive of these macrocycles being electron deficient; electrochemical studies were performed on these dyads to confirm this.

Figure 3 shows DPVs of the investigated dyads while Figure S7 of the Supporting Information shows DPV of pristine SBDPiR and fulleropyrrolidine under similar solution conditions for comparison. The site of electron transfer was arrived

dx.doi.org/10.1021/ja503015f | J. Am. Chem. Soc. 2014, 136, 7571−7574

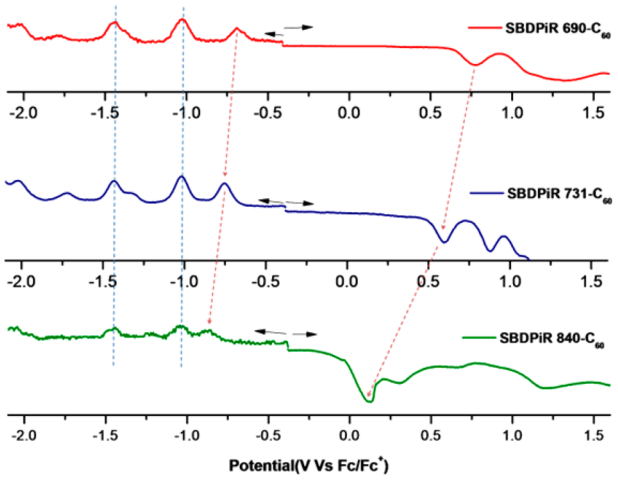

Figure 3. Differential pulse voltammograms (DPV) of SBDPiR 690-C_{60}, SBDPiR 731-C_{60}, and SBDPiR 840-C_{60} dyads in benzonitrile, 0.1 M (n-Bu_4N)ClO_4. Scan rate = 5 mV/s, pulse width = 0.25 s, and pulse height = 0.025 V. The blue dotted line shows fullerene reductions, while the red dotted arrow shows the corresponding SBDPiR's first oxidation and first reduction peaks.

by comparing the redox potentials of the control compounds. In the dyads, the first two one-electron reductions corresponding to fullerene were located at −1.02 and −1.44 V versus Fc/Fc^+, not significantly different from the control compound, 2-phenylfulleropyrrolidine.[27] The first reduction of the SBDPiR entity in the dyads was located at −0.68, −0.75, and −0.87 V, respectively, for SBDPiR 690-C_{60}, SBDPiR 731-C_{60}, and SBDPiR 840-C_{60} dyads, while the corresponding first oxidation was located at 0.77, 0.60, and 0.11 V versus Fc/Fc^+, respectively. The gradual narrowing of the HOMO−LUMO gap of the SBDPiR dyes across the series with facile oxidation was evident from these studies.

The energetics for charge separation were calculated using the redox and optical data according to Rehm−Weller's approach,[28] and the calculated values were found to be exergonic for PET via the singlet excited state of SBDPiR leading to the formation of $SBDPiR^{\bullet+}$-$C_{60}^{\bullet-}$ charge-separated states.[29] That is, the magnitudes of $-\Delta G^{S}_{CS}$ were found to be −0.11, −0.12, and −0.47 eV, respectively, for the SBDPiR 690-C_{60}, SBDPiR 731-C_{60}, and SBDPiR 840-C_{60} dyads. Such calculations also ruled out the possibility of $SBDPiR^{\bullet-}$-$C_{60}^{\bullet+}$ formation because of their higher-energy states. An energy level diagram showing the main photochemical events is shown in Figure S8 in the Supporting Information.

Further, femtosecond and nanosecond transient absorption spectral studies were performed to gather evidence for the occurrence of PET and to secure kinetic information on charge separation and charge recombination. For this, first, transient spectra of the SBDPiR probes in benzonitrile were recorded. As shown in Figure S9 in the Supporting Information, immediately after excitation with 100 fs flash at 400 nm in benzonitrile, the spectra showed the absorption of the singlet SBDPiR in the form of bleaching at 708 nm for SBDPiR 690, and at 732 and 758 nm for SBDPiR 731. The decay of the singlet excited states was accompanied by populating the triplet excited states (see Figure S10 of the Supporting Information for nanosecond transient spectra of SBDPiR derivatives). However, for SBDPiR 840 having electron donating N,N-dimethylamino groups, the spectral features were that of fast charge separation.

The transient absorption spectral changes were distinctly different for the dyads; that is, spectral features corresponding to the occurrence of ultrafast charge separation were observed. Figure 4 shows the spectral changes recorded at different time

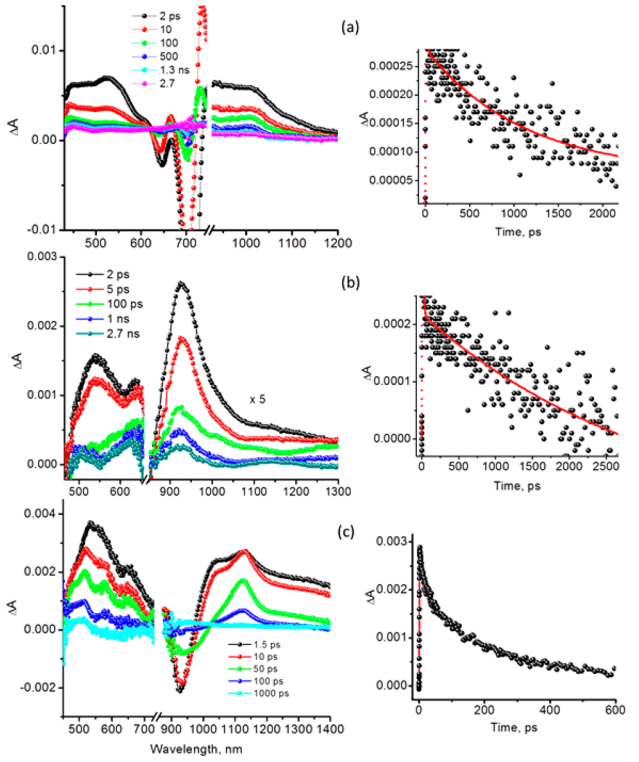

Figure 4. Femtosecond transient spectra at the indicated time intervals of SBDPiR 690-C_{60}, SBDPiR 731-C_{60}, and SBDPiR 840-C_{60} dyads in benzonitrile. The samples were excited using 400 nm 100 fs laser pulses. The decay profile of the $C_{60}^{\bullet-}$ at 1020 nm is shown in the right panels for a while for (b and c); the decay profile of $SBDPiR^{\bullet+}$ at 917 and 1130 nm is shown.

intervals. Transient bands to the formation of $SBDPiR^{\bullet+}$ in the near-IR region and around 1020 nm corresponding to the formation $C_{60}^{\bullet-}$ were observed. In order to identify the cation radical of the SBDPiR, the probes were chemically oxidized, as shown in Figure S11 of the Supporting Information. In the case of SBDPiR 690, the main band corresponding to $SBDPiR^{\bullet+}$ appeared at 756 nm, while this band for SBDPiR 731 and SBDPiR 840 was located at 810 and 1024 nm, respectively. As shown in Figure 4a for SBDPiR 690-C_{60} dyad, bands in the 850−960 nm region corresponding to $SBDPiR^{\bullet+}$ and at 1020 nm corresponding to $C_{60}^{\bullet-}$ were observed, establishing charge separation in the dyad. The kinetics of charge separation, k_{CS} (estimated from the rise time constant) and charge recombination, k_{CR} calculated from the decay profile of the $C_{60}^{\bullet-}$ band (Figure 4a, right panel) were found to be 1.10×10^{11} and 7.66×10^{8} s^{-1}, respectively. For SBDPiR 731-C_{60} dyad, the cation peak expected at 810 nm overlapped with the overtone band of the excitation band, while the $C_{60}^{\bullet-}$ band appeared as a shoulder to the 925 nm transient band (Figure 4b). The k_{CS} and k_{CR} calculated from the decay profile of the anion radical (Figure 4b, right panel) were found to be 1.12×10^{11} and 9.78×10^{8} s^{-1}, respectively. In the case of SBDPiR 840-C_{60}, both cation and anion bands having the same absorption maxima, appeared at 1020 nm (Figure 4c). For calculating the k_{CS} and k_{CR} values, the time profile of this band

dx.doi.org/10.1021/ja503015f | J. Am. Chem. Soc. 2014, 136, 7571−7574

was utilized. The measured k_{CS} and k_{CR} were found to be 7.14 × 10^{10} and 2.93 × 10^{9} s^{-1}, respectively. The estimated errors in the kinetic values are not more than ±10%. The charge recombination proceeded in populating the triplet state of the sensitizers prior to returning to the ground state, as witnessed from the developing triplet features at higher timescales in the femtosecond transient spectra in Figure 4.

In summary, the present work reports the synthesis and characterization of three new donor−acceptor dyads derived from thieno-pyrrole-fused BODIPY and fullerene. The SBDPiR macrocycle in these dyads acted as near-IR sensitizers and revealed ultrafast photoinduced electron transfer (PET) to the covalently linked fullerene as revealed by femtosecond transient absorption studies. The charge recombination was 1−2 orders of magnitude slower, a predicted trend for fullerenes due to their low reorganization energy demand in electron transfer reactions.[30] The present class of dyads is important not only for harvesting light energy from the near-IR region but also in building optoelectronic devices operating under near-IR light as the excitation source. Further studies along this line are in progress in our laboratories.

■ ASSOCIATED CONTENT

Supporting Information

Synthetic, experimental, and complete citation details of ref 26; Maldi-mass and IR; HOMO and LUMO orbitals of dyads; DPV of pristine SBDPiR and fulleropyrrolidine; an energy level diagram showing photochemical events; and spectra of femtosecond and nanosecond transient and chemically oxidized SBDPiR probes. This material is available free of charge via the Internet at http://pubs.acs.org.

■ AUTHOR INFORMATION

Corresponding Author

E-mail: youngjae-you@ouhsc.edu; Francis.DSouza@UNT.edu

Notes

The authors declare no competing financial interest.

■ ACKNOWLEDGMENTS

This work was supported by the National Science Foundation (Grant 1110942 to F.D.) and OCAST (HR11-58 to Y.Y.).

■ REFERENCES

(1) *Photoinduced Electron Transfer*; Fox, M. A., Chanon, M., Eds.; Elsevier: Amsterdam, 1988; Part A−D.

(2) *Electron Transfer in Chemistry*; Balzani, V., Ed.; Wiley-VCH: Weinheim, 2001, Vols. *1*−*5*.

(3) Gust, D.; Moore, T. A.; Moore, A. L. *Acc. Chem. Res.* **2009**, *42*, 1890−1898.

(4) Fukuzumi, S.; Kojima, T. *J. Mater. Chem.* **2008**, *18*, 1427−1439.

(5) Fukuzumi, S.; Ohkubo, K.; D'Souza, F.; Sessler, J. L. *Chem. Commun.* **2012**, *48*, 9785−9940.

(6) Wasielewski, M. R. *Acc. Chem. Res.* **2009**, *42*, 1910−1921.

(7) Sanchez, L.; Martín, N.; Guldi, D. M. *Angew. Chem., Int. Ed.* **2005**, *44*, 5374−5382.

(8) Bottari, G.; de la Torre, G.; Guldi, D. M.; Torres, T. *Chem. Rev.* **2010**, *110*, 6768−6816.

(9) El-Khouly, M. E.; Ito, O.; Smith, P. M.; D'Souza, F. *J. Photochem. Photobiol. C* **2004**, *5*, 79−104.

(10) D'Souza, F.; Ito, O. *Chem. Soc. Rev.* **2012**, *41*, 86−96.

(11) Tkachenko, N. V.; Lemmetyinen, H. In *Handbook of Carbon Nanomaterials*, D'Souza, F.; Kadish, K. M., Eds.; World Scientific Publications: Singapore, 2011; Chapter 13, pp 405−440.

(12) Dualeh, A.; Delcamp, J. H.; Nazeeruddin, M. K.; Grätzel, M. *Appl. Phys. Lett.* **2012**, *100*, 173512−173514.

(13) Arunkumar, E.; Ajayaghosh, A. *Chem. Commun.* **2005**, *5*, 599−601.

(14) Loudet, A.; Burgess, K. *Chem. Rev.* **2007**, *107*, 4891−4932.

(15) Umezawa, K.; Nakamura, H.; Makino, D.; Citterio, D.; Suzumi, K. *J. Am. Chem. Soc.* **2008**, *130*, 1550−1551.

(16) Kamkaew, A.; Lim, S. H.; Bee, H. B.; Kiew, L. Y.; Chung, L. Y.; Burgess, K. *Chem. Soc. Rev.* **2013**, *42*, 77−88.

(17) Awuah, S. G.; You, Y. *RSC Adv.* **2012**, *2*, 11169−11183.

(18) Ulrich, G.; Ziessel, R.; Harriman, A. *Angew. Chem., Int. Ed.* **2008**, *47*, 1184−1201.

(19) El-Khouly, M. E.; Fukuzumi, S.; D'Souza, F. *ChemPhysChem* **2014**, *15*, 30−47.

(20) Imahori, H.; Norieda, H.; Yamada, H.; Nishimura, Y.; Yamazaki, I.; Sakata, Y.; Fukuzumi, S. *J. Am. Chem. Soc.* **2001**, *123*, 100−110.

(21) Engelhardt, V.; Khuri, S.; Fleischhauer, J.; Garcia-Iglesias, M.; Gonzalez-Rodriguez, D.; Bottari, G.; Torres, T.; Guldi, D. M.; Faust, R. *Chem. Sci.* **2013**, *4*, 3888−3892.

(22) Awuah, S. G.; Das, S. K.; D'Souza, F.; You, Y. *Chem.—Asian J.* **2013**, *8*, 3123−3132.

(23) Amin, A. N.; El-Khouly, M. E.; Subbaiyan, N. K.; Zandler, M. E.; Fukuzumi, S.; D'Souza, F. *Chem. Commun.* **2012**, *48*, 206−208.

(24) Bandi, V.; El-Khouly, M. E.; Ohkubo, K.; Nesterov, V. N.; Zandler, M. E.; Fukuzumi, S.; D'Souza, F. *J. Phys. Chem. C* **2014**, *118*, 2321−2332.

(25) Maggini, M.; Scorrano, G.; Prato, M. *J. Am. Chem. Soc.* **1993**, *115*, 9798−9799.

(26) Frisch, M. J.; Trucks, G. W.; Schlegel, H. B.; Scuseria, G. E.; Robb, M. A.; Cheeseman, J. R.; Zakrzewski, V. G.; Montgomery, J. A., Jr.; Stratmann, R. E.; Burant, J. C.; Dapprich, S.; Millam, J. M. et al. *Gaussian 03*; Gaussian, Inc.: Pittsburgh, PA, 2003.

(27) Smith, P. M.; McCarty, A. L.; Nguyen, N. Y.; Zandler, M. E.; D'Souza, F. *Chem. Commun.* **2003**, 1754−1755.

(28) Rehm, D.; Weller, A. *Isr. J. Chem.* **1970**, *7*, 259−271.

(29) $-\Delta G^{S}_{CS} = \Delta E_{0-0} - e(E_{ox} - E_{red}) - E_{sol}$, ΔE_{0-0} is the energy of the lowest excited state of SBDPiR being 1.76, 1.65 and 1.46 eV (estimated) for SBDPiR 690, SBDPiR 731, and SBDPiR 840, respectively. Symbols E_{ox} and E_{red} correspond to the first oxidation potential of SBDPiR derivatives and the first reduction potential of C_{60}, respectively. Symbol E_{sol} is electrostatic energy derived from the distance between the electron donor and acceptor using the continuum model.

(30) Imahori, H.; Hagiwara, K.; Akiyama, T.; Aoki, M.; Taniguchi, S.; Okada, T.; Shirakawa, M.; Sakata, Y. *Chem. Phys. Lett.* **1996**, *263*, 545−550.